Drug Design, Development and Therapy

Dovepress
Taylor & Francis Group

Open Access Full Text Article

ORIGINAL RESEARCH

Cinobufagin Inhibits Invasion and Migration of Non-Small Cell Lung Cancer via Regulating Glucose Metabolism Reprogramming in Tumor-Associated Macrophages

Ying Sun, Huitong Yang, Xue Mei, Jinchan Xia, Long Feng, Jianfeng Gao, Wei Jiang, Min Jiang, Xu Hao, Yilin Feng, Yunfeng Lian

Medical College, Henan University of Chinese Medicine, Zhengzhou, Henan, 450046, People's Republic of China

Correspondence: Ying Sun, Medical College, Henan University of Chinese Medicine, Zhengzhou, Henan, 450046, People's Republic of China, Email sunying0109@163.com

Background: The immunosuppressive tumor microenvironment (TME) in lung cancer, driven in part by M2-polarized tumor-associated macrophages (TAMs), contributes to worse prognosis and supports tumor progression. Cinobufagin (CB), an active compound in cinobufotalin injections, has demonstrated potential antitumor effects by modulating macrophage activity. This study investigated the mechanism by which CB influences glucose metabolism and polarization in M2 TAMs by focusing on the regulation of HIF-1α.

Methods: Human THP-1 monocytes were differentiated into M2 macrophages by stimulation with interleukin-4 at 20 ng/mL and then treated with cinobufagin at 2 μM, either alone or together with the HIF-1α activator DMOG at 1 mM. HIF-1α hydroxylation and ubiquitination were evaluated by Western blot and co-immunoprecipitation. Glycolytic activity was determined by measuring uptake of the glucose analogue 2-NBDG, extracellular lactate levels and expression of GLUT1, PKM2, LDHA and MCT1. M2 polarization markers CD206, Arg-1 and IL-10 were quantified by qRT-PCR, and TGF-β and IL-10 secretion was measured by ELISA. PD-L1 expression was assessed by Western blot, immunofluorescence and chromatin immunoprecipitation. Finally, conditioned media from treated macrophages were applied to A549 cells to evaluate migration through wound-healing assays and invasion using Transwell inserts, and to HUVECs to quantify tube formation.

Results: Using DMOG, an HIF-1α activator, we stimulated glycolysis in M2 macrophages, promoting their immunosuppressive polarization and elevating PD-L1 expression, a checkpoint protein associated with immune evasion. CB treatment reversed this effect by increasing HIF-1α hydroxylation and ubiquitination, leading to decreased HIF-1α stability, glucose uptake, and lactate production in M2 macrophages. Additionally, CB pre-treatment of M2 macrophages reduced the secretion of the cytokines TGF-β and IL-10, thereby limiting lung cancer cell migration, invasion, and angiogenesis.

Conclusion: These findings suggest that CB suppresses M2 macrophage-mediated tumor support by targeting HIF-1α and glycolysis, thereby reprogramming the TME toward an anti-tumor state. This highlights CB's potential of CB in the treatment of lung cancer by countering immunosuppressive macrophage activity.

Keywords: TAMs, metabolic reprogramming, TME, cancer immunotherapy, lung cancer

Introduction

Lung cancer is a common malignant tumor, accounting for approximately 18.7% of global cancer mortality.[1] Lung cancer has two subtypes: non-small cell lung cancer (NSCLC) and small cell lung cancer (SCLC).[2] NSCLC is the primary histological subtype, comprising adenocarcinoma, large-cell carcinoma, and squamous cell carcinoma, and is responsible for approximately 85% of all cases.[3] Traditional NSCLC treatment includes local therapy, radiotherapy, and chemotherapy. With a deeper exploration of the molecular mechanisms of tumor progression, emerging immune checkpoint inhibitors (ICIs) and small-

Received: 4 May 2025
Accepted: 21 July 2025
Published: 2 August 2025

molecule inhibitors have been widely applied in the clinical treatment of NSCLC.[4] However, less than a quarter of cases have an effective immune response, which may be related to tumor microenvironment (TME) suppression.[5] Targeting immune cells within the TME to improve the tumor immune microenvironment has become an important target and prognostic indicator in tumor treatment, which also applies to NSCLC.[6] Metabolic interventions, such as inhibiting glycolysis or modulating fatty acid oxidation, have the potential not only to directly suppress tumor growth but also to enhance the efficacy of ICIs and chemotherapy by restoring effective T cell infiltration and function within the TME.[7] Thus, targeting macrophage metabolism offers a complementary approach that can synergize with existing therapies to achieve more robust and sustained antitumor immunity.

TAMs constitute a specific population of macrophages in TME. As the primary cellular component of TME, they exert crucial functions in lung cancer tumorigenesis, remodeling of the immune microenvironment, and chemotherapy resistance and are closely associated with poor prognosis.[6,8,9] During the early stages, TAMs are predominantly activated in the classically activated M1. As nutrient levels in the TME decline, lactic acid concentration increases, a hypoxic environment forms, pH decreases, anti-inflammatory factors are released, and macrophages gradually shift from the M1 type to the alternatively activated M2 type.[9] It has been reported that M2-type TAMs can suppress the microenvironment immune status and drive metastasis by modulating matrix metalloproteinases (MMPs), growth factors, cytokines, chemokines, and other inflammatory mediators.[10–12] Clinical studies have found that M2 macrophages induce tumor metastasis and are closely correlated with poor prognosis in patients with NSCLC.[13] Reversing TAM polarization to promote the transition from the M2 to M1 phenotype can induce specific antitumor immunity and inhibit tumor metastasis.[14] Therefore, targeting TAM polarization and reprogramming the immunosuppressive M2 phenotype may be an effective strategy to improve the tumor in patients with NSCLC.

The distinctiveness of metabolites and the complexity of metabolic pathways modulate TAMs and other cell interactions, thereby influencing lung cancer progression, recurrence, and metastasis.[15,16] TAM metabolism is in a state of dynamic change, with different metabolic processes present in various subpopulations, and there is a close relationship between metabolism and phenotype.[17,18] A commonly accepted view is that M1 macrophages rely on aerobic glycolysis and the pentose phosphate pathway, resulting in a disrupted tricarboxylic acid (TCA) cycle and impaired mitochondrial function. M2 macrophages depend on oxidative phosphorylation and the oxidation of fatty acids to maintain oxidative phosphorylation and an intact TCA cycle. With TME remodeling, TAM glucose metabolism exhibits diverse characteristics: fatty acid oxidation can also occur in M1 macrophages and glycolysis can occur in M2 macrophages.[19] Recent studies have found that M2 macrophages are an immune cell subset with strong glucose uptake capability. CD206, CD301, and CD163 expression in M2 macrophages in TAMs depends on increased glycolytic flux.[20] Therefore, glycolysis in TAMs may accelerate tumor progression. A study on NSCLC found that circSHKBP1, enriched in exosomes from NSCLC cells, inhibited miR-1294 expression in THP-1 macrophages in vitro, upregulated the expression of hexokinase 2 (HK2), pyruvate kinase M2 (PKM2), and glycolytic enzyme glucose transporter 1 (GLUT1), increased glucose uptake and lactate production, and promoted M0 polarization to M2, leading to a high infiltration of M2 TAMs in NSCLC tumor tissue.[21] Another clinical study found that elevated GLUT1 expression in lung squamous cell carcinoma tissues was associated with poorer survival rates and worse pathological responses to adjuvant immunochemotherapy.[22] Thus, targeting glycolysis may be an effective method for reprogramming TAMs to treat NSCLC.

Hypoxia-inducible factor-1α (HIF-1α) is a key upstream transcription factor involved in TAM glycolysis. Under hypoxic conditions, HIF-1α activates TAM glycolysis, promoting HK2, PKM2, GLUT1, and lactate dehydrogenase A (LDHA) expression, which converts pyruvate into lactate.[23] Studies have found that HIF-1α and GLUT1 are co-expressed in tumor-infiltrating macrophages, and GLUT1-mediated macrophage glycolysis can induce polarization toward the M2 phenotype.[22] Therefore, understanding the regulatory mechanisms of HIF-1α in reprogramming the glucose metabolism in TAMs is particularly important. Recent studies have found that the hydroxylation and ubiquitin-proteasome degradation pathways affect HIF-1α stability. With the assistance of oxygen and α-ketoglutarate (α-KG), prolyl hydroxylase domain proteins hydroxylate HIF-1α. Hydroxylated HIF-1α undergoes ubiquitination by acting as an E3 ubiquitin ligase, VHL, resulting in its degradation.[24] Recent studies have shown that HIF-1α modulates TAM polarization and PD-L1 expression.[25] PD-L1 and HIF-1α co-expression is closely associated with poor prognosis in patients with NSCLC.[26] NSCLC-derived exosomes influence HIF-1α expression through the TLR2/NF-κB axis, increasing glucose uptake, promoting lactate release as

a glycolytic product, stimulating TAMs to express NOS2, inhibiting mitochondrial oxidative phosphorylation, and resulting in the conversion of pyruvate to lactate. Lactate further activates NF-κB, forming a positive feedback regulatory loop, inducing PD-L1 expression, and promoting the polarization of TAMs toward a pro-tumor phenotype, creating a favorable environment for tumor metastasis.[27] Additionally, PD-L1+ macrophages are the primary PD-L1-expressing cells in liver cancer tissue, and PKM2 stimulates the polarization of PD-L1+ macrophages to a pro-tumor phenotype in an HIF-1α-dependent manner. Conversely, inhibiting glycolysis can inhibit PD-L1 in TAMs, restore the ability of T cells to produce IFN-γ, and kill autologous liver cancer cells.[28] Therefore, it remains to be clarified whether HIF-1α influences TAM glycolysis through hydroxylation and ubiquitination, and whether glycolysis is involved in regulating TAM polarization and immunosuppressive phenotypes requires further exploration.

Cinobufotalin injection, which is commonly used in clinical cancer treatment, has a broad anticancer spectrum, diverse application modes, and good tolerance. Studies have found that cinobufotalin injection combined with cisplatin is effective in treating advanced NSCLC, improving patients' quality of life and reducing adverse reactions.[29] Cinobufagin (CB), a key bioactive component of cinobufotalin, exerts anti-tumor actions.[30] In clinical studies on NSCLC, cinobufagin has been used as an adjunctive agent to enhance the efficacy of conventional treatments, reduce tumor size and adverse effects, and improve quality of life.[31] CB also inhibited the growth of subcutaneous xenografts in nude mice without significant toxicity to other major organs.[32] CB has been reported to inhibit M2 polarization by modulating membrane metallo-endopeptidase (MME), blocking the FAK/STAT3 signaling pathway, significantly reducing metastatic tumor burden in breast cancer, and hindering epithelial-mesenchymal transition within tumors.[33] Recently, studies also demonstrated that CB suppressed colorectal cancer angiogenesis by disrupting the endothelial mammalian target of rapamycin/HIF-1α axis.[34] However, it remains unclear whether cinobufagin influences macrophage polarization by regulating glucose metabolic reprogramming, thereby affecting NSCLC cell invasion and migration. This study aimed to assess the effect and mechanism of action of CB, the main active ingredient of cinobufotalin, on glucose metabolism reprogramming and TAMs polarization, providing theoretical evidence for exploring CB's pharmacological effects of CB in inhibiting NSCLC cell invasion and migration and its clinical application.

Materials and Methods

Cell Culture

The human monocytic leukemia cell line, THP-1 (Cat#: FH0112), was purchased from Shanghai Fuheng Biology (Shanghai, China). The human lung adenocarcinoma cell line A549 (Cat#: CCL-185) and human umbilical vein endothelial cells (HUVEC; Cat#: CRL-1730) were obtained from the ATCC. After thawing, THP-1 cells, A549 cells, and HUVECs were cultured in RPMI-1640 medium (Cat# 31880; Solarbio) supplemented with 10% fetal bovine serum (FBS; cat# 164210; Wuhan Procell Life Science & Technology Co., Ltd.) and incubated at 37°C in a 5% CO_2 incubator.

Preparation of Conditioned Medium

The medium from macrophages in different polarization states in 6-well plates was discarded. The macrophages were then rinsed with PBS. Macrophages were then placed in serum-free medium for 24 h. The culture supernatants were collected and centrifuging at 12000×g for 15 min at 4°C. The supernatant was collected and used as conditioned medium.[35] To ensure consistency across treatment groups, the conditioned media were adjusted to match glucose, lactate, and pH levels.

Treatments

For the CB treatment, macrophages were exposed to CB (Sigma-Aldrich; 25 ng/mL) for 24 h before being prepared for subsequent experiments.[35] Similarly, for DMOG treatment, macrophages were exposed to DMOG, a HIF-hydroxylase inhibitor[36] (MedChem Express; 20 μM) for 24 h before being prepared for further experiments.

Establishment of M2 Macrophage Model

An in vitro M2 macrophage polarization model previously established by our research team was used. Phorbol 12-myristate 13-acetate (PMA; Cat#P1585; Sigma-Aldrich) was used to induce THP-1 cells to M0 macrophages, followed by induction with human IL-4 (Cat#: 200-04; PeproTech, China) to generate an M2 macrophage model. THP-1 cells were centrifuged at 1000 rpm for 5 min. After discarding the supernatant, the cells were resuspended in medium containing 200 ng/mL PMA. After continuous 24-h incubation, the medium was discarded, and the cells were collected as M0 macrophages. For M2 polarization, M0 macrophages were rinsed twice with PBS, followed by 24-h incubation with 20 ng/mL IL-4.

Quantitative Real-Time PCR (qRT-PCR)

Cellular RNA was extracted using TRIzol reagent (Cat#: 15596026; Thermo Fisher Scientific). RNA concentration was determined using a NanoDrop-2000 UV spectrophotometer. RNA samples were reverse-transcribed into cDNA using the RevertAid First Strand cDNA Synthesis Kit (Cat#: K1621; Thermo). qRT-PCR was performed using the PowerUp™ SYBR™ Green Master Mix (Cat#: A25743; Thermo Fisher Scientific). GAPDH was used as a reference and expression was determined using the $2^{-\Delta\Delta CT}$ method. The primer sequences are listed in Table 1.

Cellular Glucose Uptake

The Cell Meter 2-NBDG Glucose Uptake Assay Kit (Cat#23500; AAT Bioquest) was used to detect the cellular glucose uptake. To prepare the 2-NBDG staining solution, five microliters of 2-NBDG (10 mg/mL) was added to assay Buffer I (1/5 mL) and mixed thoroughly. The supernatant was then removed without disturbing the cells. 2-NBDG staining solution (100 µL/well, 96-well plate) was added. The cells were incubated with 2-NBDG (34 µg/mL) at 37°C for 20 min to allow for sufficient glucose uptake. After incubation, 2-NBDG was removed, washed with assay buffer I, and incubated in 100 µL of Assay Buffer II. A fluorescence microscope with a fluorescein isothiocyanate (FITC) filter was used to monitor the fluorescence signal, characterizing glucose uptake in macrophages by fluorescence intensity.

Colorimetric Detection of Lactic Acid Concentration in Supernatant

A lactic Acid (LA) Colorimetric Assay Kit (Cat#:E-BC-K044-M; Elabscience) was used to measure lactic acid concentration in the cell culture supernatant. The macrophage culture supernatant from each group was collected in a centrifuge tube and centrifuged at 10,000g for 10 min at 4 °C. The supernatant was stored on ice for subsequent use. Standard solutions with different concentrations were prepared according to the manufacturer's instructions. Five microliters of the sample and different concentrations of the standard solution were then added to the respective wells. One hundred and twenty microliters of chromogenic reagent was added, mixed thoroughly, and incubated at 37°C for 5 min, followed by incubation with stop solution. After thorough mixing for 5s using a microplate reader, the optical density (OD) value was measured at 530 nm.

Table 1 Primer Sequences

Gene	Forward	Reverse
CD206	CTACAAGGGATCGGGTTTATGGA	TTGGCATTGCCTAGTAGCGTA
Arg-1	CTGTGGGAAAAGCAAGCGAG	CATGGCCAGAGATGCTTCCA
IL-10	GGTTGCCAAGCCTTGTCTGA	AGGGAGTTCACATGCGCCT
GLUT1	GGCCAAGAGTGTGCTAAAGAA	ACAGCGTTGATGCCAGACAG
PKM2	ATGTCGAAGCCCCATAGTGAA	TGGGTGGTGAATCAATGTCCA
LDHA	GCAGACTTGGCTGAGAGCAT	TGGGACACTGAGGAAGACATC
MCT1	ATGATCGCTGGTGGTTGTCT	CAAGTTGAAAGCAAGCCCAA
GAPDH	TCCAAAATCAAGTGGGGCGA	AGTAGAGGCAGGGATGATGT

Western Blot

Cells were lysed in RIPA lysis buffer (Cat#: R0010; Solarbio) containing protease and phosphatase inhibitors (Cat#: P0100; Solarbio) was added to each well. Protein concentrations were measured utilizing BCA method and the proteins were denatured. Protein samples were run on a 10% SDS polyacrylamide gel and transferred to a polyvinylidene fluoride (PVDF) membrane. The PVDF membranes were blocked with 5% BSA (Millipore Sigma) for 2 h at room temperature. The membranes were incubated at 4°C with the following primary antibodies: GLUT1 (1:1000; Cat#: AF5462; Affinity Biosciences), LDHA (1:1000; Cat#: DF6280; Affinity Biosciences), PKM2 (1:1000; Cat#: DF6280; CST), MCT1 (1:5000; Cat#: GTX129599-S; GeneTex), HIF-1α (1:5000; Cat#: 66730-1-Ig; Proteintech), Hydroxy-HIF-1α (1:1000; Cat#: 3434T; CST), and GAPDH (1:10000; Cat#: GTX100118; GeneTex) overnight. After washing with TBST, the membranes were incubated with goat anti-rabbit (1:10000; Cat#: SA00001-1; Proteintech) or goat anti-mouse (1:10000; Cat#: SA00001-2; Proteintech) antibodies at room temperature for 1 h. After washing, ECL kit (Cat#: PE0010; Solarbio) was used for imaging. Grayscale values were quantified using ImageJ software.

Co-Immunoprecipitation

After protein extraction from the cells using RIPA lysis, the protein concentration was determined using the BCA method. The antibodies used were HIF-1α (1:1000; Catalog No. 36169; CST) and ubiquitin (Catalog No. 3936; CST). Add 1.0 μg IgG and 20 μL of protein A/G beads (thoroughly mixed before use) were added to the protein supernatant of the negative control (IgG) group, and 20 μL of protein A/G beads was directly added to the experimental group and incubated with rotation at 4°C for 1 h. The mixture was centrifuged at 2000 g at 4°C for 5 min, and the supernatant was collected and incubated overnight at 4°C. Then, 80 μL of protein A/G beads were added, gently mixed by flicking, and incubated at 4°C for 2 h. The mixture was centrifuged at 2000 g for 5 min at 4°C, and the supernatant was carefully aspirated to ensure that the beads at the bottom were undisturbed to collect the immune complex. The immune complex was washed four times with 1 mL pre-chilled IP lysis buffer, centrifuging at 2000 g at 4°C for 5 min, and the supernatant discarded. After the last wash, 80 μL of 1× reducing buffer was added and the mixture was boiled for 10 min and centrifuged at 1000 g at 4°C for 5 min. The supernatant was collected for Western blotting analysis.

Immunofluorescence

The immunofluorescence was performed according to previous study.[37] The cells were fixed in 4% paraformaldehyde for 30 min and then washed twice for 3 min each. Cells were permeabilized with 0.5% Triton X-100 at room temperature for 10 min, followed by blocking with protein-free rapid blocking solution for 15 min at room temperature. After the blocking solution was discarded, the wells were washed with PBS 3 times. Primary antibodies anti-HIF-1α (1:200; Cat# 66730-1-Ig; Proteintech) or anti-PD-L1 (1:100; Cat# 17952-1-AP; Proteintech) were added followed by overnight incubation at 4°C. Next, the primary antibody was aspirated, the dishes were washed 3 times with PBS, and the respective secondary antibodies Dylight 594 (1:200; Cat#: A23420; Abbkin) or Dylight 488 (1:200; Cat#: A23210; Abbkin) were added and incubated in the dark for 1 h. Subsequently, the dishes were washed 3 times with PBS, stained with 10 μg/mL DAPI in the dark for 5 min, and washed four times with PBS. Images were captured using a confocal laser microscope.

Enzyme-Linked Immunosorbent Assay (ELISA)

After collecting the culture supernatant from each group of cells, the secretion levels in the cell culture supernatant were measured using IL-10 (Cat#: MM-0066H1; Meimian) and TGF-β (Cat#: MM-1774H1; Meimian) ELISA detection kits.

Chromatin Immunoprecipitation (ChIP)

Cells from each group were collected and cross-linked with formaldehyde. DNA fragments were sonicated to obtain 100–500 bp fragments. HIF-1α antibody (1:5000; Cat#: 66730-1-Ig; Proteintech) was added to immunoprecipitate the cross-linked protein-DNA complexes. The complexes were then immunoprecipitated, eluted, de-crosslinked, and the DNA products were purified and recovered. Primers for the PD-L1 gene were designed using Primer Premier 5.0, and synthesized by Sangon

Biotech, Shanghai (Forward: AAGGAAAGGCAAACAACGA; Reverse: GCCCAAGATGACAGACGAT). DNA enrichment levels were analyzed using qRT-PCR. The $2^{-\Delta\Delta CT}$ method was used to calculate the enrichment of PD-L1 gene promoter fragments, with the input group serving as an internal control.

Wound-Healing Assay

Macrophage-conditioned medium was thawed and mixed with RPMI-1640 medium containing 1% FBS. When the cells adhered and reached approximately 90% confluence, a vertical scratch was made using a 200 μL pipette tip. The medium was removed, and the wells were washed with PBS to remove detached cells from the scratch. Fresh mixed medium was then added to the plates. The cells were then incubated for an additional 24 hours. Images were captured under an optical microscope, and the results were analyzed using the ImageJ software. The cell migration rate was calculated as (scratch width at 0 h − scratch width at 24 h) / scratch width at 0 h × 100%.

Invasion Assay

A 6-well Transwell chamber with an 8 μm pore size was used for the cell invasion assay. The matrix gel was diluted with serum-free medium and 200 μL gel was added to each well, followed by incubation in an incubator for 30 min. Cells were prepared at a density of 5×10^5 cells/mL. A 6-well plate with transwell chambers was prepared, 2 mL of the cell suspension was added to the upper chamber, and 2 mL prepared macrophage-conditioned medium was added to the lower chamber. The setup was placed in an incubator for incubation. After 24 h, the 6-well plate was removed and the cells in the upper chamber were removed with a cotton swab. Invading cells were fixed with 4% paraformaldehyde for 30 min, stained with 0.1% crystal violet dye at room temperature for 25 min, rinsed with PBS to remove excess dye, and air dried at room temperature. Cells were photographed under an inverted microscope, and cell counting was performed using the ImageJ software.

Tube Formation Assay

A549 cells were seeded in 6-well plates at a density of 1×10 cells/well. Macrophage-conditioned medium was mixed with DMEM in a 1:1 ratio, added to a 6-well plate, and incubated for 24 h. The supernatant was collected, centrifuged at 1000 rpm for 5 min, and stored at −80°C. To maintain sterility, the 96-well plate, pipette, and pipette tips were pre-cooled, and the matrix gel was placed in an ice bath at 4°C overnight. The next day, 50 μL of the matrix gel was added to a pre-cooled 96-well plate, gently tapped to spread the gel evenly, and placed in an incubator for 30 min to solidify. HUVEC in the logarithmic growth phase were digested, counted, and seeded onto a pre-coated matrix gel (2×10^4 cells per well). Conditioned medium (200 μL of conditioned medium was added to each well and the 96-well plate was incubated for 6 h. Tube formations were photographed under an inverted microscope, and statistical analysis was performed using ImageJ software.

Statistical Analysis

Experimental data were analyzed using GraphPad Prism 9.5, presented as mean ± standard deviation. Due to small sample sizes (n=3), significant differences between different treatment groups were evaluated using permutation tests. Statistical significance was set at $p < 0.05$.

Results

Actions of CB on M2 Macrophage-Related Genes

The qRT-PCR results showed that the compared to M0 macrophages, CD206, Arg-1, and IL-10 were higher in M2 macrophages. After CB treatment, the CD206, Arg-1, and IL-10 levels in M2 macrophages were downregulated (Figure 1A–C). These results indicated that CB is involved in the modulation of M2 macrophage polarization.

Effect of CB on Glycolysis in M2 Macrophages

The activation of glycolysis can induce TAMs polarization towards the M2 phenotype, promoting tumor progression.[28] First, we used immunofluorescence to detect fluorescence in macrophages after the uptake of 2-NBDG, with the

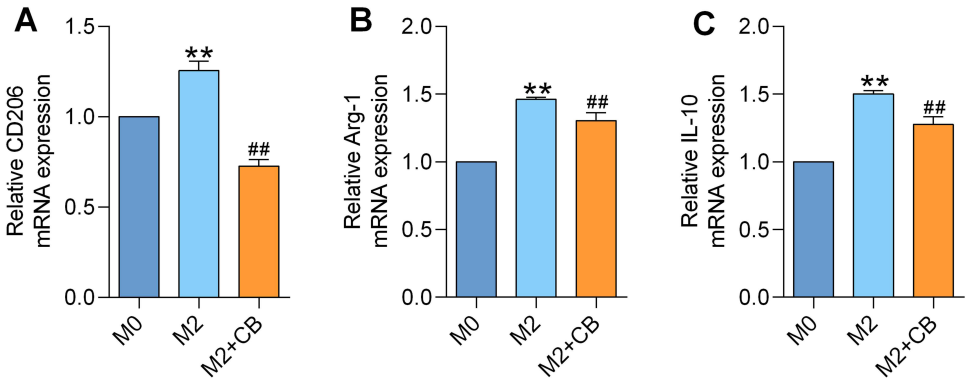

Figure 1 Effect of CB on Genes Related to M2 Macrophage Polarization. (**A**–**C**) Real-time quantitative PCR analysis of mRNA levels for CD206, Arg-1, and IL-10; n=3; ***P*<0.01 compared to M0; ##*P*<0.01 compared to M2.

fluorescence intensity representing glucose uptake by macrophages. The results showed that the fluorescence intensity was higher in the M2 macrophages than in the M0 macrophages. After 24 h of CB treatment, the fluorescence intensity of the M2 macrophages decreased (Figure 2A and B). A colorimetric assay was used to measure the concentration of lactate, a glycolytic product, in M2 macrophage supernatant. The results indicated that lactate concentration was higher

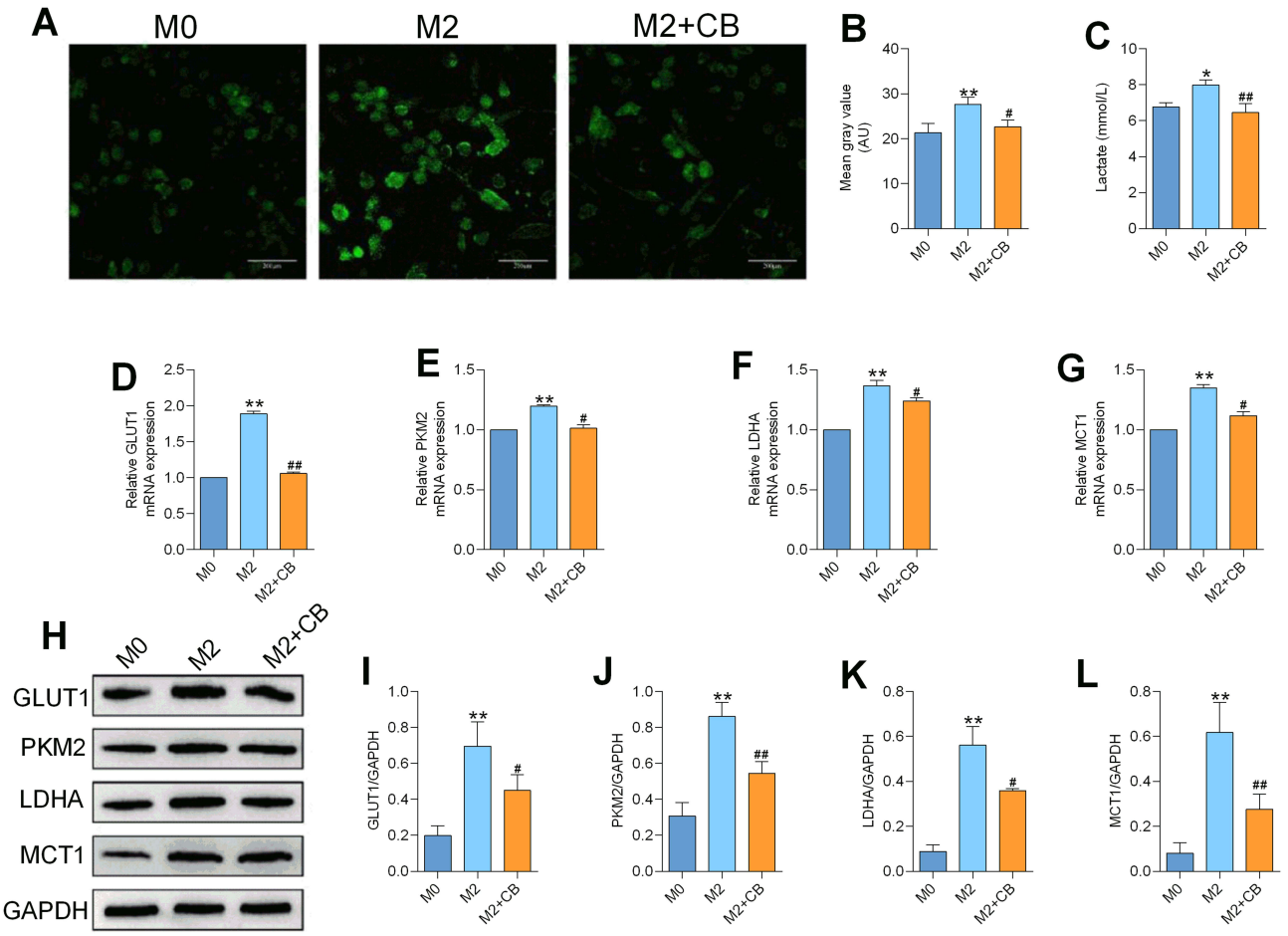

Figure 2 Effect of CB on Glycolysis in M2 Macrophages. (**A**) Fluorescence images of macrophages after uptake of 2-NBDG (400×); (**B**) Quantification of average fluorescence intensity; (**C**) Colorimetric measurement of lactate concentration. (**D**–**G**) Real-time quantitative PCR analysis of mRNA levels for GLUT1, PKM2, LDHA, and MCT1; (**H**–**L**) Western blot analysis of protein expression levels for GLUT1, PKM2, LDHA, and MCT1. n=3; **P*<0.05, ***P*<0.01 compared to M0; #*P*<0.05, ##*P*<0.01 compared to M2.

https://doi.org/10.2147/DDDT.S531190

in the M2 macrophage culture supernatant than in the M0 group. After CB treatment, lactate concentration in the M2 macrophage culture supernatant decreased (Figure 2C). Additionally, the glycolysis-related genes GLUT1, PKM2, LDHA, and MCT1 were elevated in M2 macrophages compared to M0; in contrast, these levels were decreased in the M2+CB group compared to M2 (Figure 2D–L). These results suggested that CB regulates glycolysis in M2 macrophages.

Effects of CB on the Transcription Factor HIF-1α in M2 Macrophages

HIF-1α is a key upstream transcription factor in macrophage glycolysis that can upregulate glycolysis-related proteins and promote lactate secretion, the end product of glycolysis.[23] HIF-1α mRNA and protein levels were elevated in M2 macrophages compared to M0 macrophages. However, it is noteworthy that after CB treatment, HIF-1α mRNA levels in the M2 group increased, whereas its protein expression decreased compared to that in M0 (Figure 3A–C). The inconsistency between the transcriptional and translational levels of HIF-1α in M2 macrophages suggests that CB is involved in the regulation of the post-translational modification of HIF-1α. Studies have found that Hydroxylation and ubiquitin-proteasome degradation can affect HIF-1α stability.[24] HIF-1α activator (DMOG) is a competitive HIF-1α prolyl

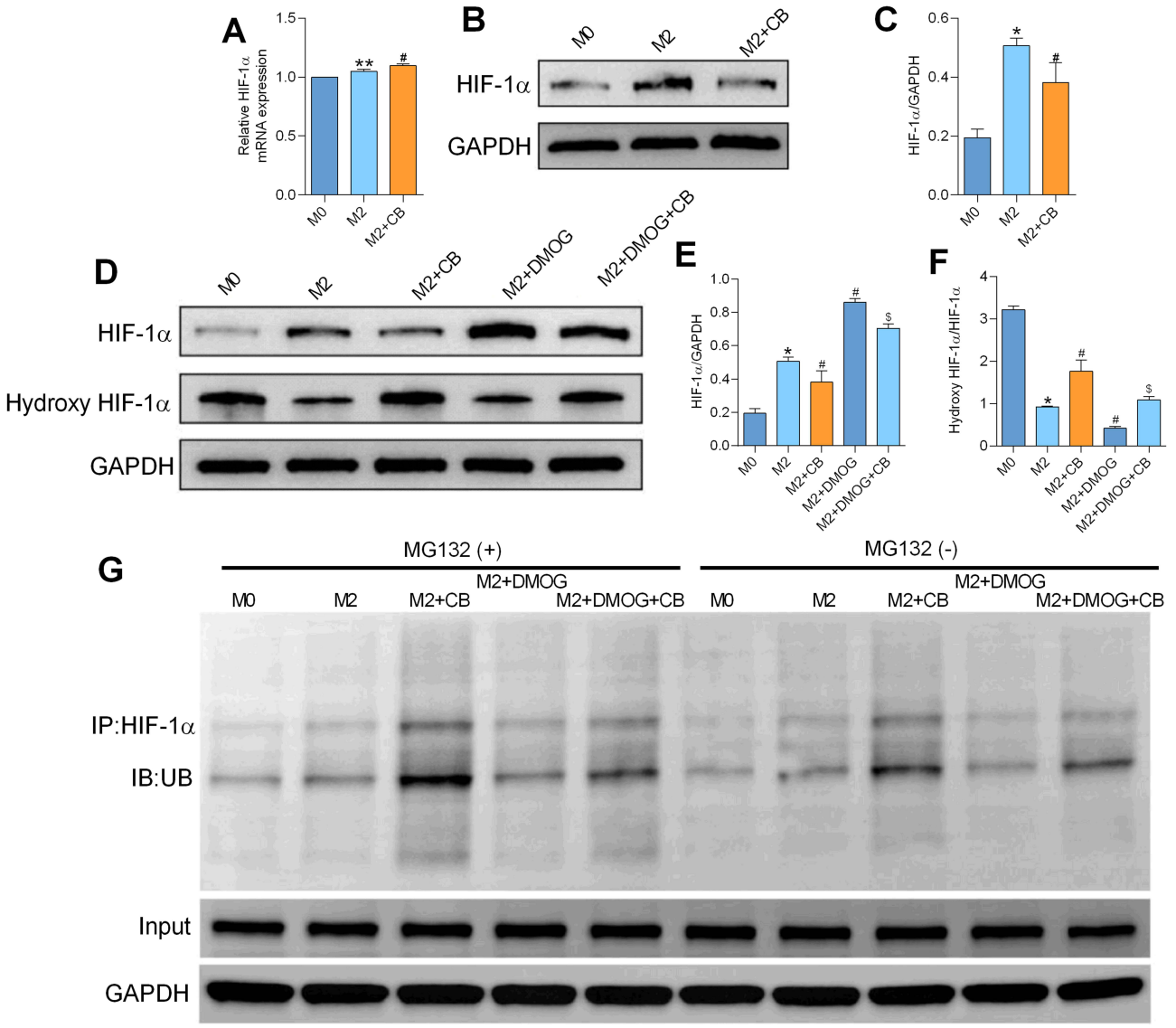

Figure 3 Effect of CB on the Transcription Factor HIF-1α in M2 Macrophages. (**A**) Real-time quantitative PCR analysis of HIF-1α mRNA levels; (**B** and **C**) Western blot analysis of HIF-1α protein expression; (**D–F**) Western blot analysis of HIF-1α and Hydroxy-HIF-1α protein expression; (**G**) Immunoprecipitation analysis of HIF-1α ubiquitination levels. n=3; **P*<0.05, ***P*<0.01 compared to M0; #*P*<0.05 compared to M2; $*P*<0.05 compared to M2+DMOG.

hydroxylase inhibitor that functions by inhibiting HIF-1α hydroxylation to enhance its stable expression. The HIF-1α hydroxylation level in M2 macrophages was lower than that in M0 macrophages, and DMOG treatment further reduced the HIF-1α hydroxylation level in M2 macrophages, while CB intervention increased HIF-1α hydroxylation levels in M2 macrophages (Figure 3D–F). Immunoprecipitation was performed to detect HIF-1α ubiquitination in M2 macrophages. HIF-1α ubiquitination was reduced in M2 macrophages compared with M0 macrophages. After DMOG treatment, HIF-1α ubiquitination in M2 macrophages is attenuated. However, following CB treatment, HIF-1α ubiquitination was upregulated in M2 macrophages (Figure 3G). Additionally, after treatment with the proteasome inhibitor MG132, HIF-1α ubiquitination in macrophages increased with consistent trends across groups (Figure 3G). These data imply that the regulatory actions of CB on HIF-1α may be mediated by the hydroxylation, ubiquitination, and proteasomal degradation pathways.

CB Targets HIF-1α to Regulate Glycolysis in M2 Macrophages

As shown in Figure 4A and B, HIF-1α nuclear translocation increased in M2 macrophages compared to that in M0 macrophages. CB intervention reduced HIF-1α levels in the M2 macrophage nuclei, whereas DMOG intervention elevated nuclear HIF-1α levels in M2 macrophages (Figure 4A and B). Additionally, CB intervention reversed the DMOG-induced increase in HIF-1α nuclear levels in the M2 macrophages (Figure 4A and B). Next, we examined glycolysis-related indicators in M2 macrophages treated with DMOG. DMOG increased glucose uptake (Figure 4C and D), promoted lactate secretion (Figure 4E), and upregulated HIF-1α and glycolysis-related proteins including GLUT1, PKM2, LDHA, and MCT1 (Figure 4F–J). However, after CB pretreatment, DMOG-induced increases in glucose uptake and lactate secretion were inhibited, and the levels of the glycolysis-related proteins GLUT1, PKM2, LDHA, and MCT1 were reduced (Figure 4C–J). These findings indicate that the effect of CB on glycolysis in M2 macrophages is mediated by regulation of the transcription factor HIF-1α.

CB Targets HIF-1α to Regulate the Expression of M2 Macrophage-Associated Factors

The activation of glycolysis can induce TAMs polarization toward the M2 phenotype, promoting tumor progression.[38] We used the HIF-1α activator DMOG to treat M2 macrophages and examined polarization-related indicators. RT-qPCR results showed that after DMOG treatment, the M2 macrophage marker CD206 and the tumor immunosuppressive factors Arg-1 and IL-10 were elevated (Figure 5A–C). After CB pretreatment, the levels of CD206, Arg-1, and IL-10 were reduced. ELISA was performed to measure IL-10 and TGF-β secretion from the culture supernatant of M2 macrophages. The results showed that TGF-β and IL-10 secretion levels were higher in the M2 macrophages than in the M0 macrophages. The M2+CB group exhibited reduced TGF-β and IL-10 secretion compared to the M2 group, whereas the M2+DMOG group showed increased secretion of these cytokines. Furthermore, compared to the M2 +DMOG group, the M2+ DMOG + CB group showed decreased TGF-β and IL-10 secretion (Figure 5D and E). These findings indicate that CB can regulate glycolysis to inhibit macrophage polarization toward the M2 phenotype.

CB Targets HIF-1α to Modulate PD-L1 in M2 Macrophages

Studies have shown that activation of glycolysis can increase immune checkpoint PD-L1 levels, thereby affecting the antitumor immune response. Next, we used the HIF-1α activator (DMOG) to treat M2 macrophages and examined PD-L1 expression. PD-L1 protein expression levels in M2 macrophages were higher than in M0 macrophages, and DMOG stimulation further elevated PD-L1 levels in M2 macrophages. After CB treatment, PD-L1 protein expression in M2 macrophages reduced (Figure 6A and B). Immunofluorescence experiments revealed that PD-L1 expression was higher in M2 macrophages than that in M0 macrophages. CB treatment reduced PD-L1 expression in M2 macrophages, whereas DMOG increased it. Additionally, CB treatment reversed the DMOG-induced increase in PD-L1 expression in M2 macrophages (Figure 6C and D).

Research has shown that HIF-1α binds to the PD-L1 promoter to regulate its expression. In this study, we used the JASPAR database to predict the binding of HIF-1α to the PD-L1 promoter, and performed chromatin immunoprecipitation assays to detect HIF-1α binding to the PD-L1 promoter. The results showed that CB treatment reduced the binding of HIF-1α to the PD-L1 promoter in M2 macrophages, whereas DMOG treatment increased this binding. CB intervention

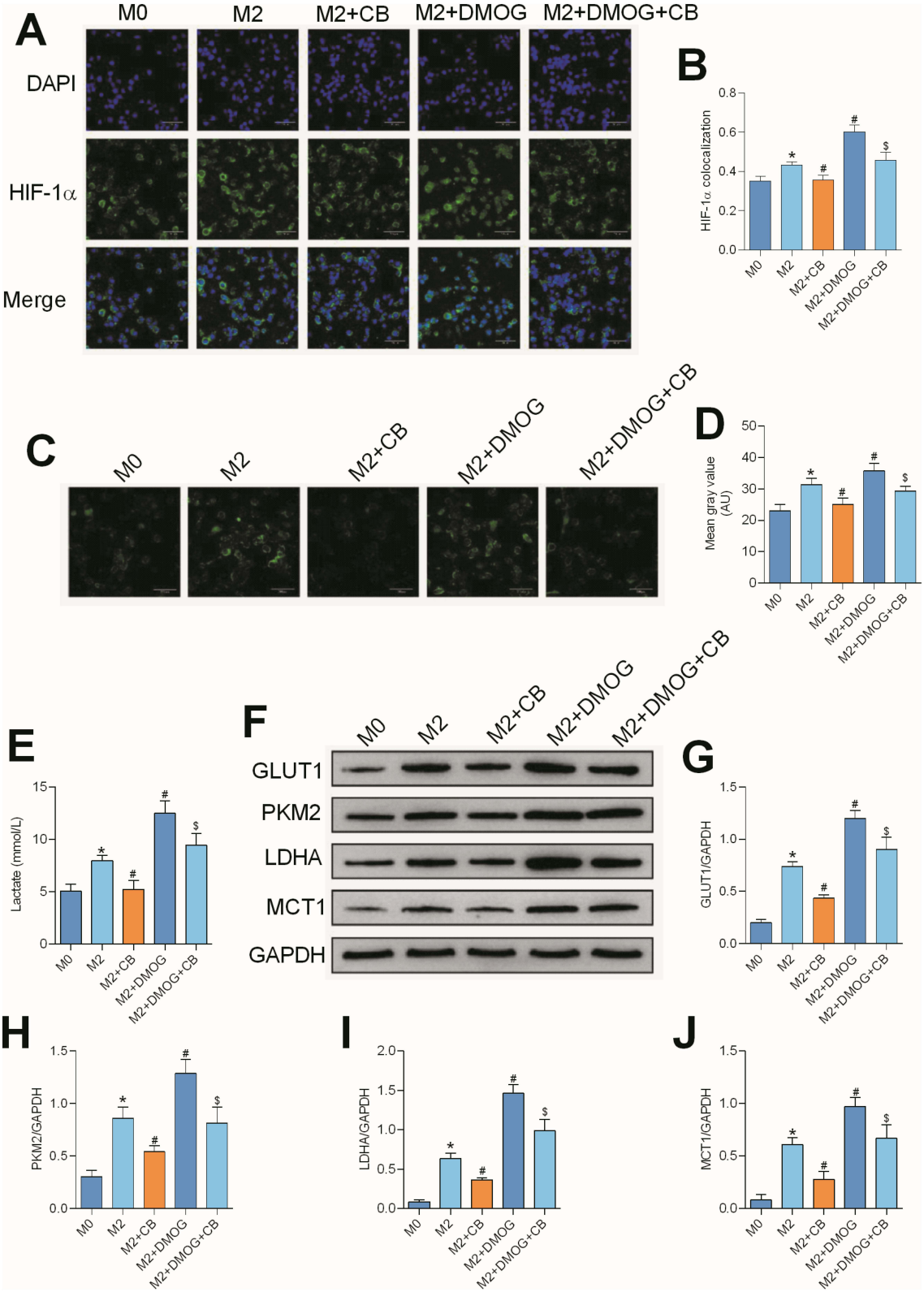

Figure 4 Effect of CB on the Transcription Factor HIF-1α in M2 Macrophages. (**A** and **B**) Immunofluorescence analysis of HIF-1α nuclear translocation (400×); (**C** and **D**) Fluorescence images of macrophages after uptake of 2-NBDG (400×); (**E**) Colorimetric measurement of lactate concentration; (**F–J**) Western blot analysis of protein expression levels for GLUT1, PKM2, LDHA, and MCT1. n=3; **P*<0.05 compared to M0; #*P*<0.05 compared to M2; $*P*<0.05 compared to M2+DMOG.

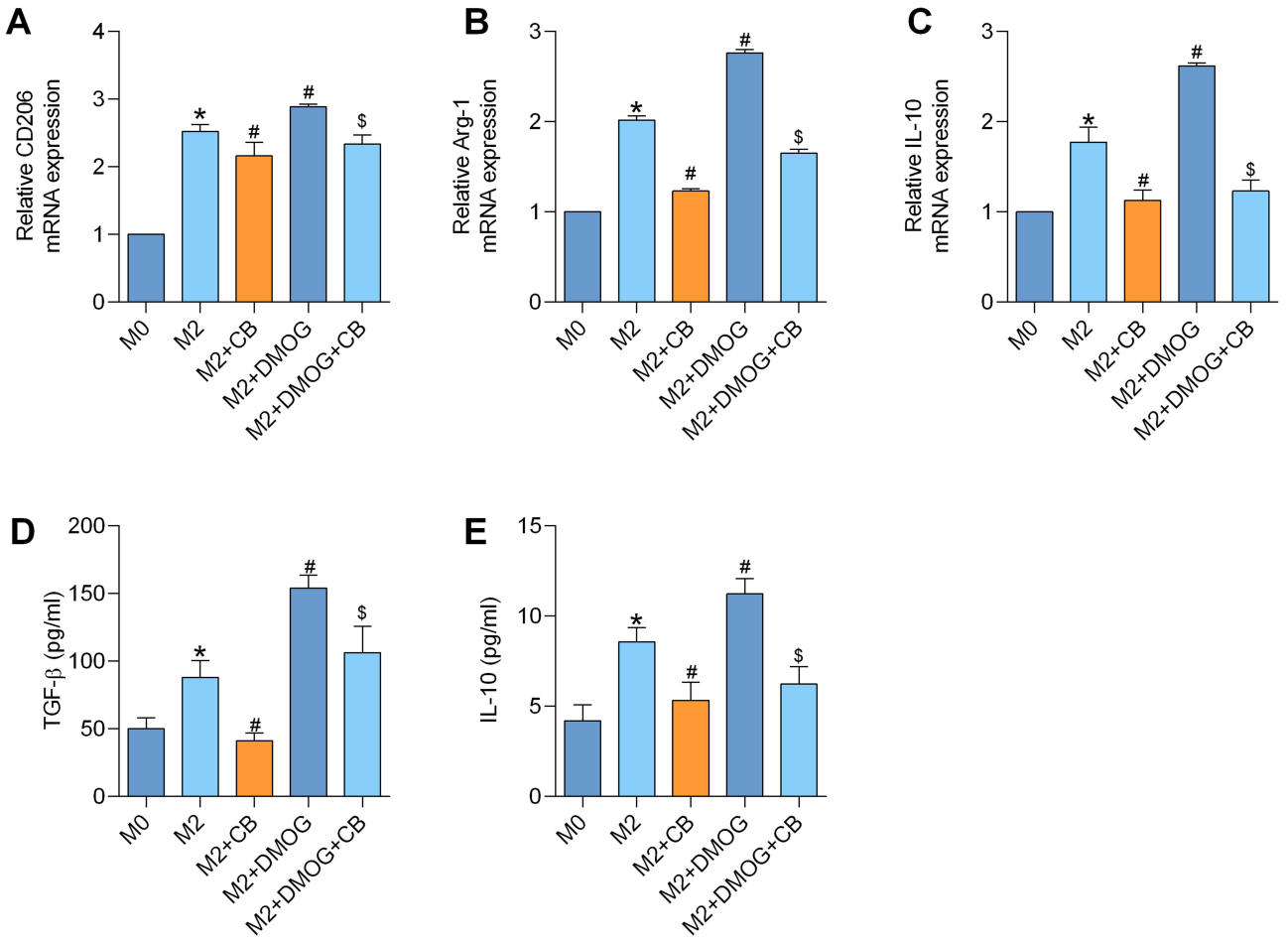

Figure 5 CB Targets HIF-1α to Regulate M2 Macrophage Polarization. (**A**–**C**) Real-time quantitative PCR analysis of mRNA levels for CD206, Arg-1, and IL-10; (**D** and **E**) ELISA measurement of TGF-β and IL-10 secretion levels. n=3; *P<0.05 compared to M0; #P<0.05 compared to M2; $$P$<0.01 compared to M2+DMOG.

reversed the DMOG-induced increase in HIF-1α binding to the PD-L1 promoter in M2 macrophages (Figure 6E and F). These findings imply that PD-L1 in M2 macrophages is regulated by the transcription factor HIF-1α, and that CB inhibits PD-L1 in M2 macrophages, possibly by targeting HIF-1α to influence glucose metabolism reprogramming.

Effect of CB-Treated Macrophage Conditioned Medium on A549 Cell Migration, Invasion, and Pro-Angiogenic Capacity

High infiltration of M2 macrophages into tumor tissues is associated with a poor prognosis in patients with NSCLC.[13] Studies have shown that M2 macrophages promote metastasis and enhance pro-angiogenic capacity by releasing matrix metalloproteinases, growth factors, cytokines, chemokines, and other inflammatory mediators.[39] A549 cells were cultured in conditioned medium from CB-pretreated macrophages and A549 cell migration was assessed using a scratch assay. Conditioned medium from M2 macrophages enhanced A549 cell migration compared to M0. Compared to M2, the migration rate of A549 cells in the M2+ CB-conditioned medium group decreased, whereas it significantly increased in the M2+ DMOG-conditioned medium group. Furthermore, compared to the M2+DMOG group, the migration rate of A549 cells in the M2+ DMOG + CB-conditioned medium group was significantly decreased (Figure 7A and B).

Invasion assay results also showed that compared to the M0 group, A549 cell invasion capacity was increased in the M2 conditioned medium. Compared to the M2 group, the A549 cell invasion capacity decreased in the M2+ CB-conditioned medium group and increased in the M2+ DMOG-conditioned medium group. Compared to the M2+DMOG group, A549 cell invasion capacity decreased in the M2+ DMOG + CB-conditioned medium group (Figure 7C and D).

https://doi.org/10.2147/DDDT.S531190

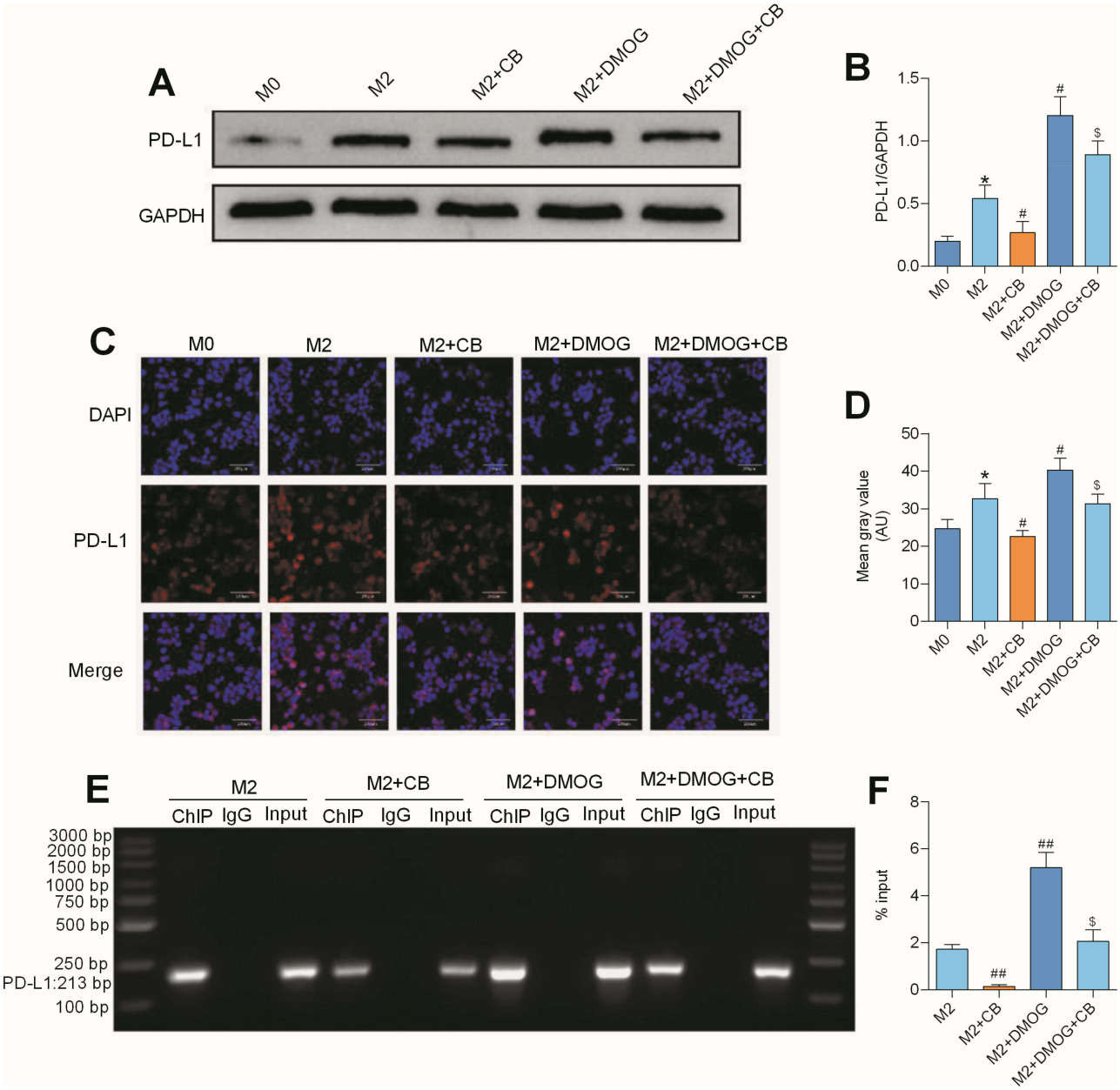

Figure 6 CB Targets HIF-1α to Regulate PD-L1 Expression in M2 Macrophages. (**A** and **B**) Western blot analysis of PD-L1 protein expression; (**C** and **D**) Immunofluorescence analysis of PD-L1 fluorescence intensity (400×); (**E** and **F**) Agarose gel electrophoresis of Input, IgG, and ChIP results. n=3; **P*<0.05 compared to M0; #*P*<0.05, ##*P*<0.01 compared to M2; $*P*<0.05 compared to M2+DMOG.

A549 cells were cultured in conditioned medium from CB-pretreated macrophages, and the supernatant was collected to treat HUVEC and observe angiogenesis. Compared with M0, the number of tubes and intersections in HUVEC increased in the M2 group. Compared with M2, the number of tubes and intersections in HUVECs decreased in the M2 +CB group and increased in the M2+DMOG group. Compared with the M2+DMOG group, the number of tubes and intersections in HUVEC decreased in the M2+DMOG+CB group (Figure 7E–G). These data imply that CB may inhibit metastasis and pro-angiogenic capacity of NSCLC cells by regulating glycolysis in M2 macrophages.

Discussion

Lung cancer is a common malignant tumor in clinical practice and the leading cause of cancer-related mortality in China. The immunosuppressive state of TME directly affects metastasis and angiogenesis in lung cancer. However, lung cancer

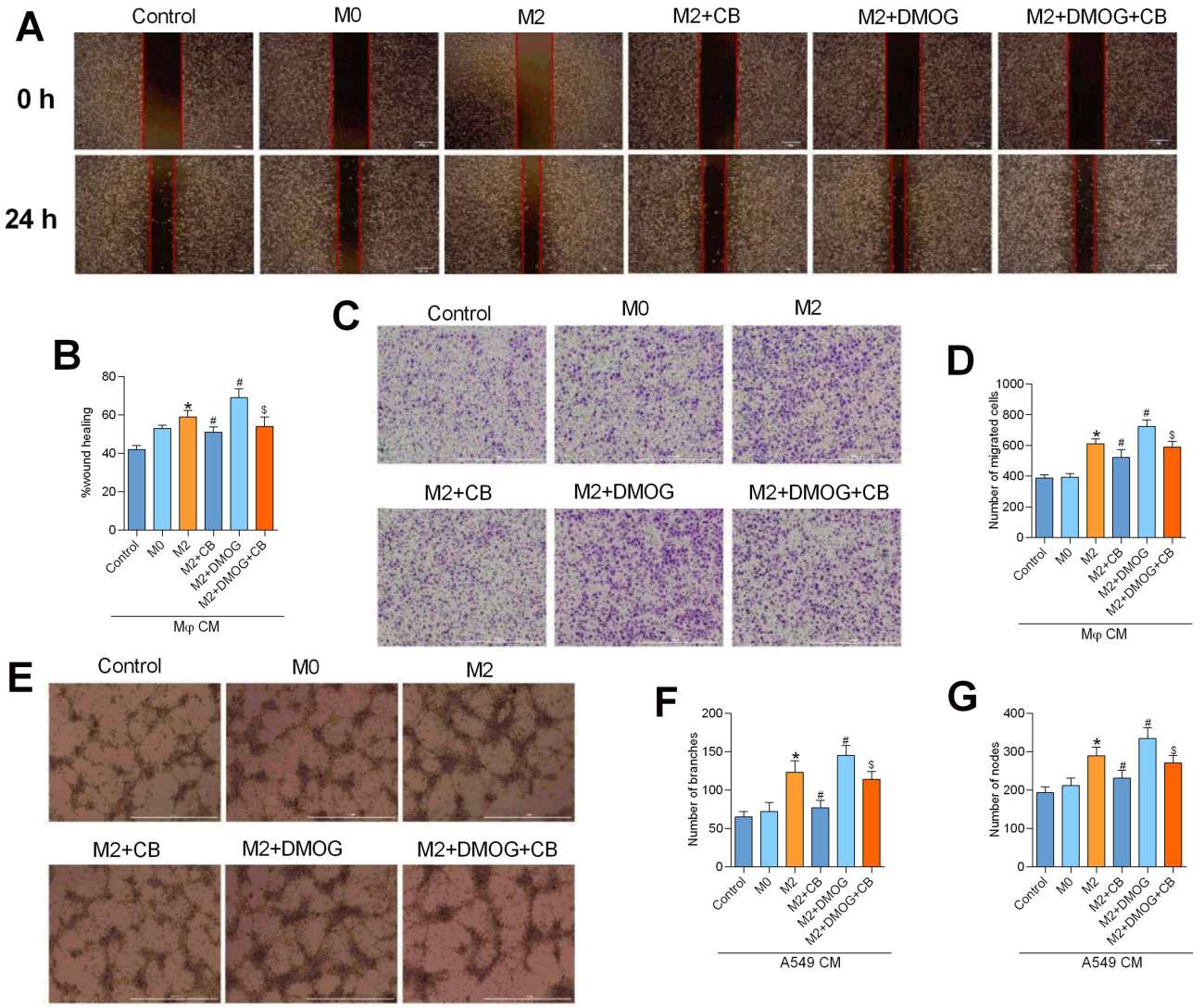

Figure 7 Effect of CB-Treated Macrophage Conditioned Medium on A549 Cell Migration, Invasion, and Pro-Angiogenic Capacity. (**A** and **B**) Scratch wound healing assay to evaluate the effect of different treatments on A549 cell migration; scale bar = 200 μm; (**C** and **D**) Transwell invasion assay to assess the impact of different treatments on A549 cell invasion; scale bar = 1000 μm; (**E-G**) Tube formation assay to examine the effect of different treatments on A549 cell pro-angiogenic capacity; scale bar = 1000 μm. n=3; **P*<0.05 compared to M0; #*P*<0.05 compared to M2; $*P*<0.05 compared to M2+DMOG.

treatment remains hampered by inadequate drug targeting, systemic toxicity, and radioresistance within the tumor microenvironment. A recent "macrophage missile" platform adsorbs peroxymonosulfate-loaded metal-organic framework nanoparticles onto live macrophages to enhance tumor homing and oxygen-independent ROS generation while minimizing premature drug release.[40] Nano-assisted radiotherapy strategies such as high-Z radiosensitizers, microenvironment-modifying nanoparticles, and biomimetic cell carriers have shown promise in boosting radiotherapy efficacy and overcoming hypoxia-driven resistance.[41] Recently, a self-assembled DNA nanomachine coupled with a MUC1 aptamer enables portable, single-cell–level detection of circulating tumor cells, offering rapid, bedside monitoring to guide personalized therapy.[42] TAMs are the main immune cells within the TME, and exert a dual regulatory action in promoting and inhibiting tumors by modulating the immune environment. The polarization of TAMs toward the M2 phenotype is closely related to treatment resistance and poor prognosis in lung cancer patients.[43] Studies have shown that the TME induces metabolic reprogramming in TAMs, affecting their polarization.[44] Metabolic processes are present within TAM clusters and there is a close relationship between metabolism and phenotypic characteristics. Among them, glucose metabolism reprogramming is involved in regulating macrophage polarization toward the M2 phenotype.[45]

https://doi.org/10.2147/DDDT.S531190

CB, a key bioactive component of cinobufotalin injection, is commonly used in clinical antitumor treatments and has a broad anticancer spectrum, diverse applications, and good tolerance. Although CB has demonstrated significant antitumor effects, the precise mechanisms are not yet fully understood. Current research on the antitumor mechanisms of CB has mainly focused on inhibiting tumor progression and attenuating apoptosis, with limited studies on its effects on tumor metastasis and TME modulation. Previous studies by our team have shown that CB can inhibit tumor growth in a Lewis lung cancer ectopic subcutaneous transplantation model in mice, reducing M2-type TAMs and increasing M1-type TAMs in tumor tissues,[35] suggesting that CB's antitumor actions of CB may be correlated with the regulation of TAM polarization. Based on the remarkable clinical antitumor actions of cinobufotalin, this study aimed to reveal the effects and mechanisms of CB on TAM glucose metabolism reprogramming and polarization, providing theoretical evidence for exploring the pharmacological actions and clinical applications of CB.

As lung cancer progresses, the M2 phenotype becomes the primary TAM subtype within the TME and its high infiltration is closely linked to low survival rates in patients with cancer. TAMs exhibit a "Warburg effect" similar to that of tumor cells, characterized by a shift to aerobic glycolysis for rapid energy production.[46] This high glycolytic metabolism is associated with TAM polarization toward the immunosuppressive M2 phenotype.[47] However, whether CB's mechanism of action of CB involves the regulation of macrophage glucose metabolism reprogramming remains unknown. No studies have yet reported the regulation of macrophage glucose metabolism by CB. Given CB's inhibitory effect of CB on M2 macrophage polarization, and the link between glucose metabolism and M2 macrophage polarization, we investigated the effect of CB on glucose metabolism reprogramming in M2 macrophages.

In this study, THP-1 cells were induced into M0 macrophages using PMA, and further polarized into M2 macrophages using human IL-4, thereby successfully establishing an in vitro macrophage polarization model. During glycolysis, glucose is transported into cells by GLUT1, converted into pyruvate by glycolytic enzymes, such as HK2 and PKM2, and then transformed into lactate by lactate dehydrogenase A (LDHA). Lactate is transported extracellularly by monocarboxylate transporters MCT4 and MCT1.[47] To further clarify the regulatory effects of CB on glucose metabolism reprogramming in M2 macrophages, we examined glucose uptake, lactate secretion, and glycolysis-related gene expression in M2 macrophages. Glucose uptake and lactate secretion were elevated in M2 macrophages compared to M0 macrophages, and the glycolysis-related genes GLUT1, PKM2, LDHA, and MCT1 were elevated, which is consistent with previous reports. After CB treatment, glucose uptake and lactate secretion were reduced in M2 macrophages, along with downregulation of glycolysis-related proteins. This implies that CB exerts actions in inhibits glycolysis in M2 macrophages by regulating glucose metabolism reprogramming.

HIF-1α is a key upstream transcription factor in macrophage glycolysis, upregulating glycolysis-related genes such as GLUT1, HK2, PKM2, and LDHA and promoting the conversion of pyruvate to lactate.[23] Our data indicate that HIF-1α mRNA and protein levels were increased in M2 macrophages, with CB treatment upregulating HIF-1α mRNA while downregulating its protein expression. The discrepancy between HIF-1α transcriptional and translational levels suggests that CB regulates HIF-1α via post-translational modifications. Hydroxylation, which affects HIF-1α stability, was investigated using the HIF-1α activator, DMOG, a competitive inhibitor of HIF-1α prolyl hydroxylase. Consistent with previous reports, DMOG reduced HIF-1α hydroxylation in M2 macrophages, increasing protein expression. CB treatment significantly increased HIF-1α hydroxylation and reduced protein expression, suggesting that CB may influence HIF-1α stability by enhancing its hydroxylation. In addition, hydroxylated HIF-1α is typically degraded via the ubiquitin-proteasome pathway under normoxic conditions.[24] Immunoprecipitation analysis showed that CB treatment increased HIF-1α ubiquitination and reduced the total protein expression.

Immunofluorescence assays showed that DMOG treatment increased HIF-1α nuclear translocation in M2 macrophages, whereas CB pretreatment partially inhibited this effect. Taken together, these findings suggest that CB inhibits M2 macrophage glycolysis by increasing HIF-1α hydroxylation and ubiquitination, thereby affecting HIF-1α stability. We further used DMOG to stimulate M2 macrophages and examine glycolysis-related indicators. DMOG increased glucose uptake, lactate secretion, and HIF-1α and glycolysis-related protein levels in M2 macrophages, whereas CB pretreatment inhibited these effects. These findings suggested that CB inhibits M2 macrophage glycolysis by targeting HIF-1α.

Glycolysis activation can induce TAMs polarization toward the M2 phenotype and promote tumor progression.[45] Previous research has suggested that CB can inhibit glycolysis in M2 macrophages; however, its impact on macrophage polarization requires further investigation. Using the HIF-1α activator, DMOG, on M2 macrophages, we assessed polarization-related markers. The results showed that DMOG treatment increased the M2 macrophage marker CD206 and immunosuppressive factors Arg-1 and IL-10, as well as the secretion of cytokines TGF-β and IL-10. This is consistent with previous findings that the activation of glycolysis promotes macrophage polarization toward the M2 phenotype. Pretreatment with CB reduced CD206, Arg-1, and IL-10 expression, and decreased the secretion of TGF-β and IL-10. These findings indicate that CB may inhibit macrophage polarization toward the M2 phenotype by regulating glycolysis.

Reports have shown that activating glycolysis not only induces TAMs to polarize toward the M2 phenotype but also increases PD-L1 expression, affecting anti-tumor immune responses and accelerating tumor progression. In liver cancer, PD-L1+ macrophages are the primary cells that express PD-L1 in the tumor tissues of patients with liver cancer and exhibit high glycolytic activity. The key glycolytic enzyme PKM2 participates in the polarization of PD-L1+ macrophages through a HIF-1α-dependent mechanism, regulating their antitumor and protumor activities. Inhibition of glycolysis can downregulate PD-L1 expression in TAMs, restoring T-cell production of IFN-γ and their ability to kill autologous liver cancer cells.[28] Thus, HIF-1α may regulate PD-L1 expression by influencing glycolysis in TAMs. Previous findings have shown that CB can enhance HIF-1α hydroxylation and ubiquitination, thereby affecting its stability and regulating glycolysis in M2 macrophages. Therefore, CB may also affect PD-L1 expression in the M2 macrophages. CB's suppression of PD-L1 in M2 macrophages offers a strong rationale for combining CB with PD-1/PD-L1 checkpoint inhibitors. By reducing macrophage-mediated immune evasion and dismantling glycolytic barriers in the TME, CB could enhance T-cell infiltration and effector function. Pairing CB with anti-PD-1/PD-L1 antibodies may therefore act synergistically to boost antitumor immunity in NSCLC. Preclinical studies in immunocompetent lung cancer models will be important to validate this strategy.

Subsequently, we used DMOG on M2 macrophages to assess PD-L1 expression. PD-L1 levels in M2 macrophages were higher than those in M0 macrophages, and DMOG stimulation further increased the PD-L1 levels in M2 macrophages. This aligns with previous findings that DMOG stabilizes HIF-1α by inhibiting prolyl hydroxylase, promoting glycolysis in M2 macrophages, and increasing PD-L1 expression. After CB treatment, PD-L1 expression in M2 macrophages decreased. These findings suggest that PD-L1 in M2 macrophages is regulated by the transcription factor HIF-1α and that CB may inhibit PD-L1 by targeting HIF-1α to influence glucose metabolism reprogramming.

Studies have shown that a high infiltration of M2 macrophages is related to poor prognosis in patients with NSCLC.[13] M2 macrophages promote metastasis and angiogenesis by releasing matrix metalloproteinases, growth factors, cytokines, chemokines, and other inflammatory mediators. Our data demonstrate that CB not only suppresses glycolysis in M2 macrophages via enhanced HIF-1α hydroxylation and ubiquitination but also markedly reduces the secretion of key immunosuppressive cytokines, TGF-β and IL-10. IL-10 is known to inhibit antigen presentation and T-cell activation, while TGF-β drives epithelial–mesenchymal transition and extracellular matrix remodeling in tumor cells, both of which facilitate immune evasion and metastasis in NSCLC.[16,48] By decreasing IL-10 and TGF-β release, CB may restore antitumor T-cell function and impair tumor cell invasiveness within the TME. Indeed, conditioned-media experiments showed that M2 macrophage–derived factors enhance A549 migration and angiogenesis, an effect reversed by CB pretreatment. These findings establish a clear mechanistic link between CB's immune-metabolic modulation of TAMs and downstream inhibition of tumor-promoting processes. Activation of HIF-1α by DMOG increases glycolysis in M2 macrophages, enhancing metastasis and angiogenesis of lung cancer cells cultured in macrophage-conditioned medium, whereas CB significantly inhibits this promotion effect. These findings suggest that CB may inhibit metastasis and angiogenesis of lung cancer cells by regulating glycolysis in M2 macrophages. From a translational standpoint, the ability of CB to destabilize HIF-1α suggests promising avenues for combination therapy. Numerous small molecules and antibodies targeting HIF-1α signaling are currently in preclinical or early clinical development for solid tumors, including NSCLC.[49,50] Co-administration of CB with HIF-1α inhibitors could achieve synergistic blockade of both macrophage glycolysis and tumor-intrinsic hypoxic adaptation, potentially overcoming resistance mechanisms that arise when either pathway is inhibited alone. However, to comprehensively map CB's direct molecular targets and validate its mechanistic network, emerging proteomic and PROTAC strategies should be employed.[51,52] These novel target-discovery approaches

will accelerate identification of critical CB targets, reveal potential resistance mechanisms, and guide rational design of optimized CB derivatives for translational development.

One limitation of the present study is the use of a relatively small sample size (n=3) for several in vitro experiments. This sample size is common in exploratory biomedical research; however, it may limit the statistical power and generalizability of the findings. To account for this, we employed non-parametric permutation tests, which are robust against violations of normality and more appropriate for small sample comparisons. A second limitation is the reliance on DMOG to stabilize HIF-1α. As a broad-spectrum 2-oxoglutarate analogue, DMOG can inhibit multiple dioxygenases beyond prolyl hydroxylases potentially eliciting off-target epigenetic or metabolic effects that do not precisely mirror physiological hypoxic signaling. Future work using complementary approaches (eg, genetic manipulation, inducible HIF-1α mutants, or controlled hypoxia) will be necessary to confirm that our observations reflect HIF-1α regulation by CB rather than broader enzyme inhibition. One additional limitation of our in vitro model is the reliance on PMA-differentiated THP-1 cells, which do not fully recapitulate the phenotype and functional heterogeneity of tissue-resident macrophages. Future studies should validate our key findings (glycolysis inhibition, cytokine secretion, PD-L1 downregulation) in primary human monocyte-derived macrophages or mouse bone marrow–derived macrophages to confirm translational relevance. Likewise, our M2 polarization protocol employed IL-4 alone; co-stimulation with IL-13 and assessment of a broader panel of M1/M2 markers would provide a more comprehensive view of macrophage phenotypes and avoid oversimplification.

Conclusions

In conclusion, CB may inhibit glycolysis in M2 macrophages by enhancing HIF-1α hydroxylation and ubiquitination, thereby impeding M2 macrophage polarization, downregulating their immunosuppressive phenotype, improving the tumor immune microenvironment, and inhibiting NSCLC invasion, migration, and angiogenesis. However, further work including in vivo efficacy studies, pharmacokinetic and toxicity profiling, and comprehensive immune-cell functional assays, is needed to confirm these findings and assess any therapeutic application.

Data Sharing Statement

Data are available upon request.

Author Contributions

All authors made a significant contribution to the work reported, whether that is in the conception, study design, execution, acquisition of data, analysis and interpretation, or in all these areas; took part in drafting, revising or critically reviewing the article; gave final approval of the version to be published; have agreed on the journal to which the article has been submitted; and agree to be accountable for all aspects of the work.

Funding

This work was financially supported by the National Nature Science Foundation of China (No. 81803863), Henan Provincial Science and Technology R&D Program Joint Fund (Advantageous Discipline Cultivation) Project (No. 242301420105), Program for Science and Technology Development of Henan Province (No. 232102311111), and Henan Provincial College Youth Key Teacher Training Program (No. 2020GGJS103).

Disclosure

The authors report no conflicts of interest in this work.

References

1. Xia C, Dong X, Li H, et al. Cancer statistics in China and United States, 2022: profiles, trends, and determinants. *Chin Med J*. 2022;135(5):584–590. doi:10.1097/CM9.0000000000002108
2. World Health Organization. Global cancer burden growing, amidst mounting need for services. 2024.
3. National Cancer Institute. SEER cancer stat facts: lung and bronchus cancer. 2022.

4. Lu Z, Xu S, Ye M, et al. Comparison of pembrolizumab plus chemotherapy versus concurrent or sequential radiochemotherapy in patients with driver mutation-lacking lung adenocarcinoma presenting with recurrent laryngeal nerve invasion leading to hoarseness. *J Clin Oncol*. 2024;42 (16_suppl):e14635. doi:10.1200/JCO.2024.42.16_suppl.e14635
5. Xing S, Hu K, Wang Y. Tumor immune microenvironment and immunotherapy in non-small cell lung cancer: update and new challenges. *Aging Dis*. 2022;13(6):1615–1632. doi:10.14336/AD.2022.0407
6. Goldberg JL, Sondel PM. Enhancing cancer immunotherapy via activation of innate immunity. *Semin Oncol*. 2015;42(4):562–572. doi:10.1053/j.seminoncol.2015.05.012
7. Cabezón-Gutiérrez L, Palka-Kotlowska M, Custodio-Cabello S, Chacón-Ovejero B, Pacheco-Barcia V. Metabolic mechanisms of immunotherapy resistance. *Explor Target Antitumor Ther*. 2025;6:1002297. doi:10.37349/etat.2025.1002297
8. Mantovani A, Allavena P. The interaction of anticancer therapies with tumor-associated macrophages. *J Exp Med*. 2015;212(4):435–445. doi:10.1084/jem.20150295
9. Sedighzadeh SS, Khoshbin AP, Razi S, Keshavarz-Fathi M, Rezaei N. A narrative review of tumor-associated macrophages in lung cancer: regulation of macrophage polarization and therapeutic implications. *Transl Lung Cancer Res*. 2021;10(4):1889–1916.
10. Wang X, Gao S, Song L, Liu M, Sun Z, Liu J. Astragaloside IV antagonizes M2 phenotype macrophage polarization-evoked ovarian cancer cell malignant progression by suppressing the HMGB1-TLR4 axis. *Mol Immunol*. 2021;130:113–121. doi:10.1016/j.molimm.2020.11.014
11. Zhu X, Liang R, Lan T, et al. Tumor-associated macrophage-specific CD155 contributes to M2-phenotype transition, immunosuppression, and tumor progression in colorectal cancer. *J Immunother Cancer*. 2022;10(9):e004219. doi:10.1136/jitc-2021-004219
12. Sumitomo R, Hirai T, Fujita M, Murakami H, Otake Y, Huang CL. M2 tumor-associated macrophages promote tumor progression in non-small-cell lung cancer. *Exp Ther Med*. 2019;18(6):4490–4498. doi:10.3892/etm.2019.8068
13. Yanagawa N, Shikanai S, Sugai M, et al. Prognostic and predictive value of CD163 expression and the CD163/CD68 expression ratio for response to adjuvant chemotherapy in patients with surgically resected lung squamous cell carcinoma. *Thorac Cancer*. 2023;14(20):1911–1920. doi:10.1111/1759-7714.14937
14. Li Z, Wang YJ, Zhou J, Umakoshi M, Goto A. The prognostic role of M2 tumor-associated macrophages in non-small-cell lung cancer. *Histol Histopathol*. 2022;37(12):1167–1175. doi:10.14670/HH-18-474
15. Liu L, Chen G, Gong S, Huang R, Fan C. Targeting tumor-associated macrophage: an adjuvant strategy for lung cancer therapy. *Front Immunol*. 2023;14:1274547. doi:10.3389/fimmu.2023.1274547
16. Huang Y, Shan G, Yi Y, et al. FSCN1 induced PTPRF-dependent tumor microenvironment inflammatory reprogramming promotes lung adenocarcinoma progression via regulating macrophagic glycolysis. *Cell Oncol*. 2022;45(6):1383–1399. doi:10.1007/s13402-022-00726-0
17. Cassetta L, Pollard JW. Targeting macrophages: therapeutic approaches in cancer. *Nat Rev Drug Discov*. 2018;17(12):887–904. doi:10.1038/nrd.2018.169
18. Yang Q, Zhang H, Wei T, et al. Single-cell RNA sequencing reveals the heterogeneity of tumor-associated macrophage in non-small cell lung cancer and differences between sexes. *Front Immunol*. 2021;12:756722. doi:10.3389/fimmu.2021.756722
19. Puthenveetil A, Dubey S. Metabolic reprogramming of tumor-associated macrophages. *Ann Transl Med*. 2020;8(16):1030. doi:10.21037/atm-20-2037
20. Reinfeld BI, Madden MZ, Wolf MM, et al. Cell-programmed nutrient partitioning in the tumour microenvironment. *Nature*. 2021;593 (7858):282–288. doi:10.1038/s41586-021-03442-1
21. Chen W, Tang D, Lin J, et al. Exosomal circSHKBP1 participates in non-small cell lung cancer progression through PKM2-mediated glycolysis. *Mol Ther Oncolytics*. 2022;24:470–485. doi:10.1016/j.omto.2022.01.012
22. Hao B, Dong H, Xiong R, et al. Identification of SLC2A1 as a predictive biomarker for survival and response to immunotherapy in lung squamous cell carcinoma. *Comput Biol Med*. 2024;171:108183. doi:10.1016/j.compbiomed.2024.108183
23. Wang T, Liu H, Lian G, Zhang SY, Wang X, Jiang C. HIF1α-induced glycolysis metabolism is essential to the activation of inflammatory macrophages. *Mediators Inflamm*. 2017;2017:9029327. doi:10.1155/2017/9029327
24. Joo HY, Jung JK, Kim MY, et al. NADH elevation during chronic hypoxia leads to VHL-mediated HIF-1α degradation via SIRT1 inhibition. *Cell Biosci*. 2023;13(1):182. doi:10.1186/s13578-023-01130-3
25. Noman MZ, Desantis G, Janji B, et al. PD-L1 is a novel direct target of HIF-1α, and its blockade under hypoxia enhanced MDSC-mediated T cell activation. *J Exp Med*. 2014;211(5):781–790. doi:10.1084/jem.20131916
26. Zheng H, Ning Y, Zhan Y, et al. Co-expression of PD-L1 and HIF-1α predicts poor prognosis in patients with non-small cell lung cancer after surgery. *J Cancer*. 2021;12(7):2065–2072. doi:10.7150/jca.53119
27. Morrissey SM, Zhang F, Ding C, et al. Tumor-derived exosomes drive immunosuppressive macrophages in a pre-metastatic niche through glycolytic dominant metabolic reprogramming. *Cell Metab*. 2021;33(10):2040–2058.e2010. doi:10.1016/j.cmet.2021.09.002
28. Lu LG, Zhou ZL, Wang XY, et al. PD-L1 blockade liberates intrinsic antitumourigenic properties of glycolytic macrophages in hepatocellular carcinoma. *Gut*. 2022;71(12):2551–2560. doi:10.1136/gutjnl-2021-326350
29. Wu W. Efficacy of Huabusu injection combined with vinorelbine and cisplatin chemotherapy in the treatment of advanced non-small cell lung cancer. *J Chronic Dis*. 2022;23(11):1718–1720.
30. Zhang G, Wang C, Sun M, et al. Cinobufagin inhibits tumor growth by inducing intrinsic apoptosis through AKT signaling pathway in human nonsmall cell lung cancer cells. *Oncotarget*. 2016;7(20):28935–28946. doi:10.18632/oncotarget.7898
31. Dai CL, Zhang RJ, An P, Deng YQ, Rahman K, Zhang H. Cinobufagin: a promising therapeutic agent for cancer. *J Pharm Pharmacol*. 2023;75 (9):1141–1153. doi:10.1093/jpp/rgad059
32. Yan S, Ma C, Zhou F, et al. Cinobufagin exerts an antitumor effect in non-small-cell lung cancer by blocking STAT3 signaling. *J Cancer*. 2023;14 (17):3309–3320. doi:10.7150/jca.86544
33. Zhu Z, Wang H, Qian X, et al. Inhibitory impact of cinobufagin in triple-negative breast cancer metastasis: involvements of macrophage reprogramming through upregulated MME and inactivated FAK/STAT3 signaling. *Clin Breast Cancer*. 2024;24(4):e244–e257.e241. doi:10.1016/j.clbc.2024.01.014
34. Li X, Chen C, Dai Y, et al. Cinobufagin suppresses colorectal cancer angiogenesis by disrupting the endothelial mammalian target of rapamycin/hypoxia-inducible factor 1α axis. *Cancer Sci*. 2019;110(5):1724–1734. doi:10.1111/cas.13988
35. Sun Y, Lian Y, Mei X, et al. Cinobufagin inhibits M2-like tumor-associated macrophage polarization to attenuate the invasion and migration of lung cancer cells. *Int J Oncol*. 2024;65(5). doi:10.3892/ijo.2024.5690

36. Singh A, Wilson JW, Schofield CJ, Chen R. Hypoxia-inducible factor (HIF) prolyl hydroxylase inhibitors induce autophagy and have a protective effect in an in-vitro ischaemia model. *Sci Rep*. 2020;10(1):1597. doi:10.1038/s41598-020-58482-w
37. Yang S, Liu H, Zheng Y, et al. The role of PLIN3 in prognosis and tumor-associated macrophage infiltration: a pan-cancer analysis. *J Inflamm Res*. 2025;18:3757–3777. doi:10.2147/JIR.S509245
38. Colegio OR, Chu NQ, Szabo AL, et al. Functional polarization of tumour-associated macrophages by tumour-derived lactic acid. *Nature*. 2014;513 (7519):559–563. doi:10.1038/nature13490
39. Zhao B, Hui X, Wang J, et al. Matrine suppresses lung cancer metastasis via targeting M2-like tumour-associated-macrophages polarization. *Am J Cancer Res*. 2021;11(9):4308–4328.
40. Liu C, Chen Y, Xu X, Yin M, Zhang H, Su W. Utilizing macrophages missile for sulfate-based nanomedicine delivery in lung cancer therapy. *Research*. 2024;7:0448. doi:10.34133/research.0448
41. Zhao L, Li M, Shen C, et al. Nano-assisted radiotherapy strategies: new opportunities for treatment of non-small cell lung cancer. *Research*. 2024;7:0429. doi:10.34133/research.0429
42. Wang Y, Shen C, Wu C, et al. Self-assembled DNA machine and selective complexation recognition enable rapid homogeneous portable quantification of lung cancer CTCs. *Research*. 2024;7:0352. doi:10.34133/research.0352
43. Hwang I, Kim JW, Ylaya K, et al. Tumor-associated macrophage, angiogenesis and lymphangiogenesis markers predict prognosis of non-small cell lung cancer patients. *J Transl Med*. 2020;18(1):443. doi:10.1186/s12967-020-02618-z
44. Zhang D, Tang Z, Huang H, et al. Metabolic regulation of gene expression by histone lactylation. *Nature*. 2019;574(7779):575–580. doi:10.1038/s41586-019-1678-1
45. Lin J, Liu Y, Liu P, et al. SNHG17 alters anaerobic glycolysis by resetting phosphorylation modification of PGK1 to foster pro-tumor macrophage formation in pancreatic ductal adenocarcinoma. *J Exp Clin Cancer Res*. 2023;42(1):339. doi:10.1186/s13046-023-02890-z
46. Mehla K, Singh PK. Metabolic regulation of macrophage polarization in cancer. *Trends Cancer*. 2019;5(12):822–834. doi:10.1016/j.trecan.2019.10.007
47. Li M, Yang Y, Xiong L, Jiang P, Wang J, Li C. Metabolism, metabolites, and macrophages in cancer. *J Hematol Oncol*. 2023;16(1):80. doi:10.1186/s13045-023-01478-6
48. Sumitomo R, Menju T, Shimazu Y, et al. M2-like tumor-associated macrophages promote epithelial-mesenchymal transition through the transforming growth factor β/Smad/zinc finger e-box binding homeobox pathway with increased metastatic potential and tumor cell proliferation in lung squamous cell carcinoma. *Cancer Sci*. 2023;114(12):4521–4534. doi:10.1111/cas.15987
49. Shirai Y, Chow CCT, Kambe G, et al. An overview of the recent development of anticancer agents targeting the HIF-1 transcription factor. *Cancers*. 2021;13(11):2813. doi:10.3390/cancers13112813
50. Araghi M, Mannani R, Heidarnejad Maleki A, et al. Recent advances in non-small cell lung cancer targeted therapy; an update review. *Cancer Cell Int*. 2023;23(1):162. doi:10.1186/s12935-023-02990-y
51. Yan S, Zhang G, Luo W, et al. PROTAC technology: from drug development to probe technology for target deconvolution. *Eur J Med Chem*. 2024;276:116725. doi:10.1016/j.ejmech.2024.116725
52. Qin S, Xiao X. Key advances and application prospects of PROTAC technologies in the next 5 years. *Future Med Chem*. 2025;17(9):987–989. doi:10.1080/17568919.2025.2498875